



Elastic modulus of nanocrystalline cemented carbide

Xue-mei LIU¹, Hai-bin WANG¹, Xiao-yan SONG¹, Riccardo MOSCATELLI²

1. College of Materials Science and Engineering, Beijing University of Technology, Beijing 100124, China;

2. Engineering Department, University of Rome “ROMA TRE”, 00146 Rome, Italy

Received 28 September 2016; accepted 26 March 2017

Abstract: The purposes of this work were to obtain the accurate elastic modulus of the nanocrystalline WC–Co cemented carbides, and to propose the mechanism for the difference of elastic modulus between the nanocrystalline and conventional polycrystalline cemented carbides. The nanocrystalline cemented carbide was prepared by spark plasma sintering (SPS) technique. The conventional polycrystalline cemented carbides were prepared by SPS and sinter-HIP techniques as references, respectively. The sintered cemented carbides were characterized by X-ray diffractometry, scanning electron microscopy and the transmission electron microscopy with precession electron diffraction technology. The elastic modulus was obtained by averaging the values measured with the continuous stiffness measurement method of the nanoindentation technology. The results show that the nanocrystalline cemented carbide has a relatively low modulus, which could be attributed to the more interface area and higher fraction ratio of the hcp cobalt phase caused by the rapid heating and cooling process during SPS.

Key words: nanocrystalline cemented carbide; elastic modulus; nanoindentation; spark plasma sintering; cobalt phase

1 Introduction

The nanocrystalline WC–Co cemented carbides (with a mean WC grain size of less than 100 nm) are proposed as candidate materials for machining tools such as printed circuit board (PCB) drills, due to their potential excellent mechanical performances [1]. Generally, the properties, such as microhardness and fracture toughness, of the nanocrystalline cemented carbides are noticed and measured using the Vickers hardness tester with a load of 300 N. Actually, the elastic modulus is another crucial factor which should be considered for the design and fabrication of the machining tools made of nanocrystalline cemented carbides. Therefore, it is very necessary to characterize the elastic modulus of the nanocrystalline cemented carbides and analyze the factors that influence this performance.

There are normally two ways to measure the elastic modulus of the conventional WC–Co cemented carbides. One is measurement of the slope of the stress–strain curve in the process of tensile loading. The other is the measurement of the speed of the ultrasound waves based

on the standards of ISO 3312–1990 and ASTM E494–2010 [2–4]. Specimens with dimensions above few millimeters in length, width and thickness direction must be satisfied in the methods. Moreover, the tensile loading and the speed of the ultrasound waves are impressible by porosity, thus the elastic modulus of the sample. However, only near full density and small dimension nanocrystalline WC–Co bulk materials have been prepared by the rapid sintering methods, such as high frequency induction-heated sintering (HFIHS) [1], spark plasma sintering (SPS) [5,6] and ultrahigh-pressure rapid hot consolidation (UPRC) [1,7] up to now. So, it is very difficult to measure the elastic modulus of the nanocrystalline cemented carbides.

In recent years, the nanoindentation technique has been well developed and recognized as a suitable method to characterize the mechanical properties of nanocrystalline bulk materials [8–10]. The hardness and elastic modulus can be measured at the nanoscale, e.g. the depth of indentation is in a range of tens of nanometers. Particularly, they are collected as a continuous function of the indentation depth by continuous stiffness measurement (CSM) method [11] under press loading and unloading process. The

nanindentation technique provides a suitable approach to investigate the mechanical properties of the nanocrystalline cemented carbides.

The aim of this work is to obtain the accurate results of the elastic modulus of nanocrystalline WC–Co cemented carbides and to explain the possible difference of elastic modulus between the nanocrystalline and conventional polycrystalline cemented carbides. Moreover, the effect of the strain rate applied during the nanindentation tests on the value of elastic modulus was concerned. The results of this work will provide a measured method for the elastic modulus of nanocrystalline ceramics and an important reference for the development of new type high-performance cemented carbides and the design of the hard-metal tools.

2 Experimental

WC–10Co cemented carbides were used as example materials in the present work. Using the nanoscale WC–Co powder as raw material, the nanocrystalline cemented carbide was prepared by SPS technique [5] at 1150 °C. For comparison, the conventional polycrystalline WC–Co cemented carbides with submicron grain size were prepared through SPS and sinter-HIP. In detail, the mixture of WC powder with the mean diameter of 6.0 μm and Co powder were sintered by SPS at 1150 °C for 5 min; the mixture of WC powder with the mean diameter of 0.2 μm and Co powder were sintered by sinter-HIP at 1420 °C for 30 min with a gas pressure of 5 MPa.

The microstructure of the nanocrystalline cemented carbide was observed by the transmission electron microscopy (TEM, JEOL JEM–2010F) with precession electron diffraction technology (Spinning Star P020, NanoMEGAS) [12]. The microstructure of the submicron grained cemented carbide was examined by scanning electron microscopy (SEM, Nova NanoSEM). The WC grain size was measured by the linear intercept method based on the images. The phase constitution of the samples was measured by X-ray diffraction. The elastic modulus was tested by the CSM method using a Berkovich diamond indenter. The maximum indentation depth was 1000 nm and the strain rate was 0.01, 0.05 and 0.1 s⁻¹, respectively. 15–20 points were measured for each sample.

3 Results and discussion

3.1 Microstructure and grain size of cemented carbide samples

The TEM micrograph and grain size distribution of the prepared nanocrystalline cemented carbide are shown in Fig. 1. It can be seen that the microstructure is homogeneous, and the WC grain size is mainly in a

range of 50–110 nm with a mean grain size of about 90 nm. The mean free path, characterizing the dimension of the cobalt phase in the cemented carbide, is 45 nm. Therefore, a nanocrystalline WC–Co material was prepared.

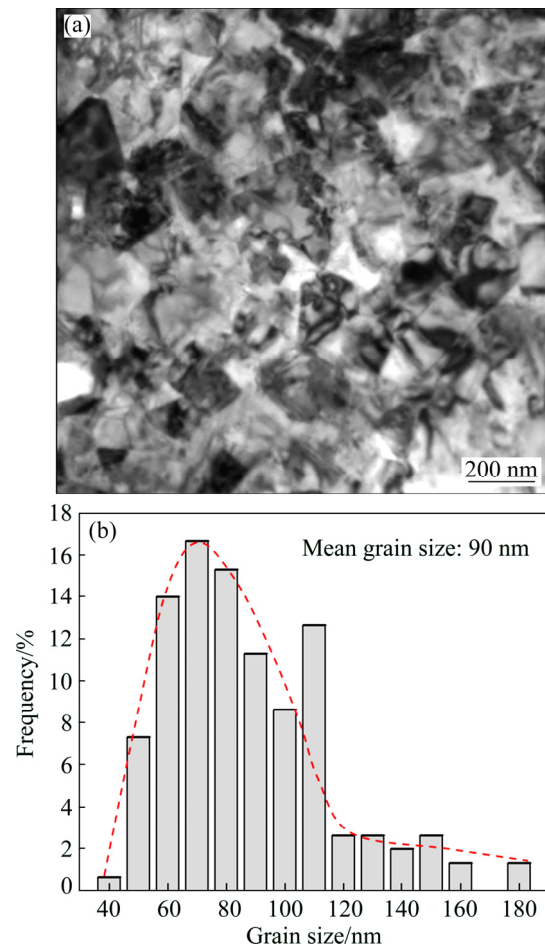


Fig. 1 Microstructure and grain size distribution of nanocrystalline cemented carbide sample prepared by in-situ reduction and carbonization reactions, and SPS method: (a) TEM image; (b) WC grain size distribution

Figure 2 shows the microstructure of the WC–10Co material prepared by sinter-HIP and SPS method, which has a relatively homogeneous grain structure with a mean grain size of about 610 nm and 1.53 μm, and the corresponding Co mean free paths are 220 nm and 396 nm, respectively.

3.2 Measurement of elastic modulus

Figure 3 shows the typical $P-h$ curves (applied indentation load versus indentation depth) of the cemented carbides by CMS method using a Berkovich diamond indenter. The loading curve can be shown by

$$P=Ch^2 \quad (1)$$

where C depends on material's property and the indenter geometry.

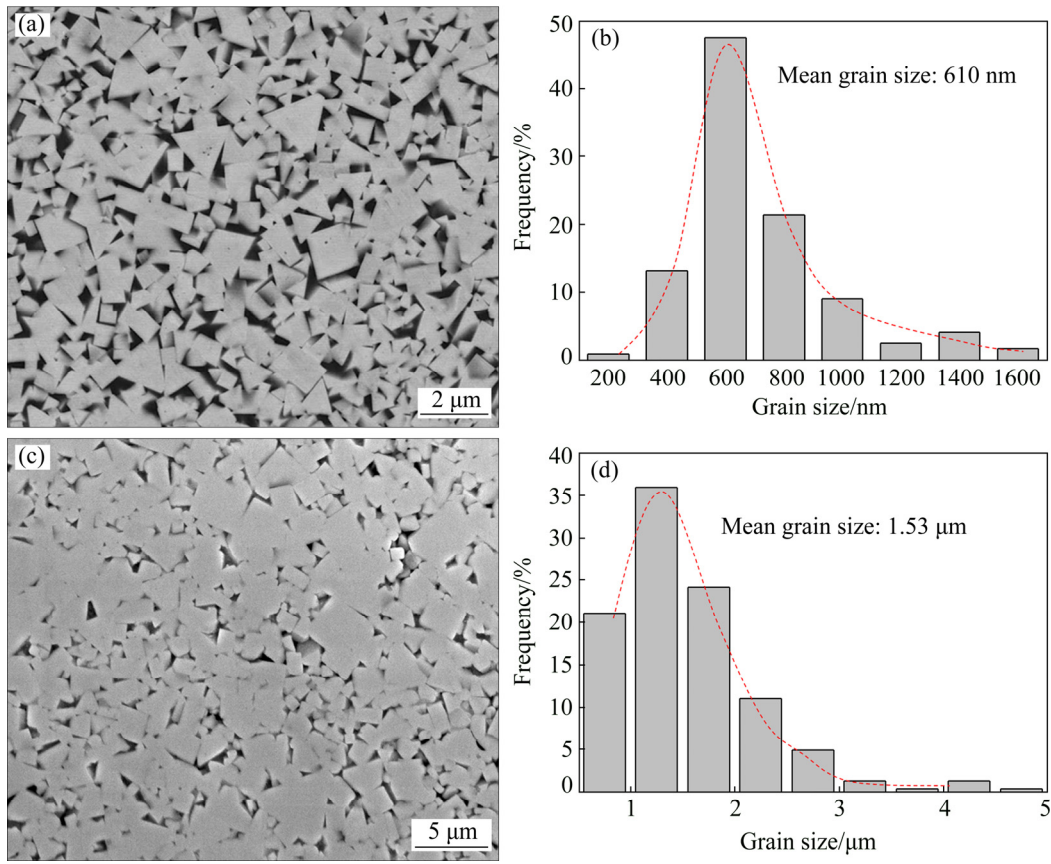


Fig. 2 Microstructure and grain size distribution of comparative WC-10Co cemented carbide prepared by different methods: (a, b) Sinter-HIP; (c, d) SPS

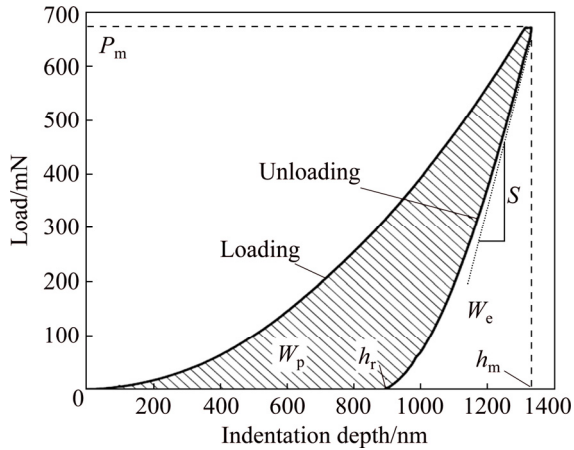


Fig. 3 Typical loading and unloading curves and energy distribution during indentation process

The unloading curves can be well approximated by the power law relation [13]:

$$P=B \times (h-h_r)^m \tag{2}$$

where B and m are the fitting parameters, and h_r is the residual depth after unloading.

The elastic modulus of the cemented carbides was measured by CMS method using a Berkovich diamond indenter. The reduced elastic modulus E_r is defined as

$$E_r = \left[\frac{1-\nu^2}{E} + \frac{1-\nu_i^2}{E_i} \right]^{-1} \tag{3}$$

where ν and ν_i are the Poisson ratios of WC-10Co and diamond indenter, respectively. The value of ν is 0.216 [14], and ν_i is 0.07 for the diamond indenter. E is the effective elastic modulus of the material and E_i is the elastic modulus of the diamond indenter. The value of E_i is 1141 GPa. The reduced elastic modulus E_r can be evaluated based on the instrumented expression, which is the function of the indenter shape (ranging from 1.0226 to 1.085, and about 1.05 for a Berkovich indenter [15]), unloading slope at the maximum indentation depth, the contact area between the indenter and the specimen. Then, the effective elastic modulus E can be obtained by Eq. (3).

At the same time, the hardness can be estimated from

$$H=P_m/A_m \tag{4}$$

where P_m is the maximum load, and A_m is the contact area between the indenter and the specimen.

Based on the effective elastic modulus results at the same indentation depth, the average elastic modulus and standard deviation were evaluated, as shown in Fig. 4.

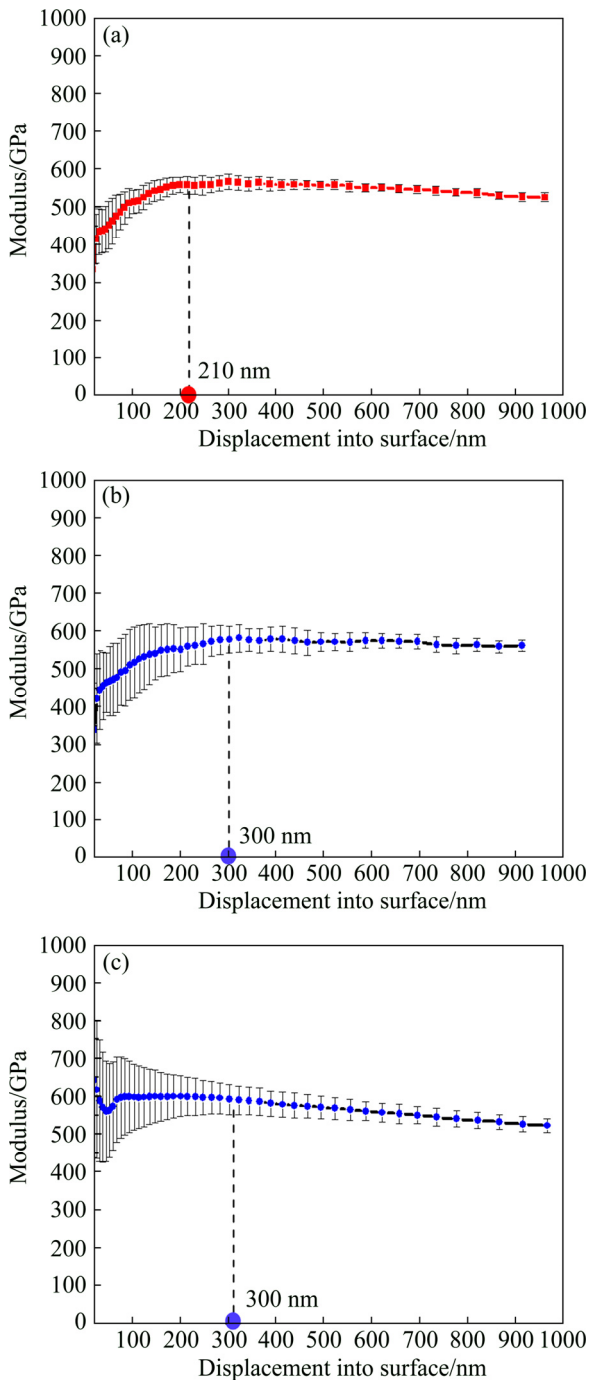


Fig. 4 Variations of elastic modulus with indentation depth for different cemented carbide samples: (a) Nanocrystalline sample; (b) Submicron grain sample sintered by HIP; (c) Submicron grain sample sintered by SPS

The average elastic modulus keeps stable and the standard derivation is less than 5% in the depth range of 210–950 nm for the nanocrystalline sample (Fig. 4(a)) and 300–950 nm for the submicron grained sample (Figs. 4(b) and (c)), respectively. The elastic modulus values are obtained by average these stable values. With the same method, the hardness values are received. As the strain rate is 0.5 s^{-1} , the elastic modulus of submicron samples sintered by SPS and sinter-HIP, and

nanocrystalline grained WC–10Co is (563.9 ± 19.05) , (588.4 ± 17.6) and (553.5 ± 13.1) GPa, and the hardness is (21.2 ± 1.08) , (18.42 ± 2.29) and (22.65 ± 1.77) GPa, respectively.

To verify the accuracy of the tested results, the elastic modulus of the prepared submicron grained WC–10Co sample was compared with the reported data of the cemented carbide samples having the same composition. As shown in Fig. 5, the elastic modulus results of submicron grained sample obtained in our experiment are in good agreement with those reported in Refs. [4,16,17].

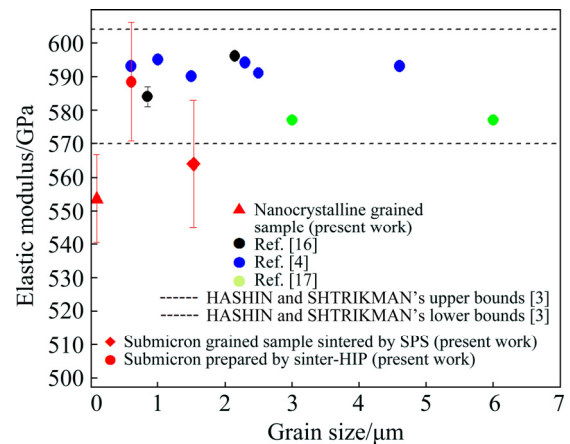


Fig. 5 Variations of elastic modulus of samples with WC grain sizes

The values of the elastic modulus are all in a range of 569.9–603.9 GPa, which is consistent with the model predicted by HASHIN and SHTRIKMAN [3]. This indicates that the CMS method is suitable to measure the elastic modulus of the prepared materials, and the values are reliable.

Compared with submicron and micron grained cemented carbides, the nanocrystalline WC–Co sample has a lower elastic modulus (with a mean value of 553.5 GPa, as shown in Fig. 5). To ensure the reliability of the elastic modulus of the nanocrystalline cemented carbides, the normal image and the Nanovision three-dimensional (3D) image of perspective view of the Berkovich indentation on the surface were characterized after unloading (as shown in Fig. 6). No pores, pile-up and sink-in were observed in the vicinity of the indentation. The present results indicate that the measured elastic modulus values of the near full density nanocrystalline WC–Co cemented carbide are reliable.

Figure 7 shows the changes of elastic modulus with strain rate applied during the nanoindentation tests. Based on the results, it can be concluded that: (1) At the higher strain rates, the elastic modulus was higher. The increase of the elastic modulus with increasing strain rate can be attributed to the sensitivity of the material to

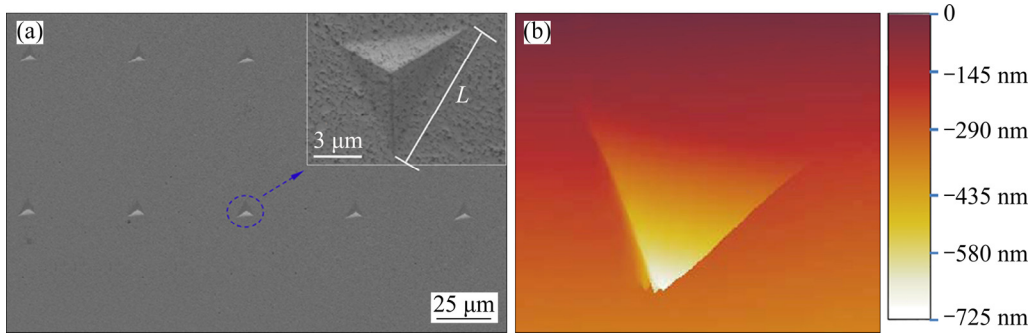


Fig. 6 Berkovich indentation on surface of nanocrystalline sample: (a) SEM image; (b) Nanovision 3D image of perspective view

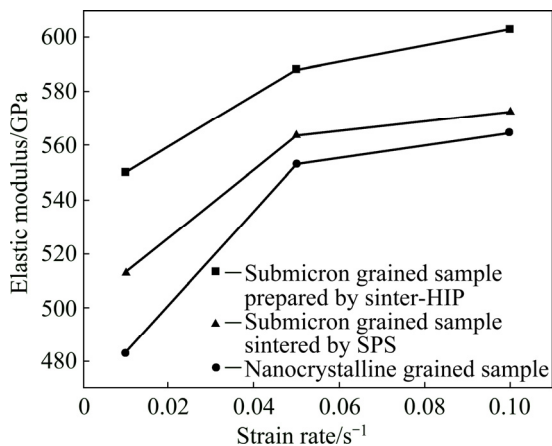


Fig. 7 Change of elastic modulus of submicron and nanocrystalline grained samples with strain rate applied during nanoindentation tests

changes of the strain rate. This effect was also observed in metals by experiments [18]. (2) At the same strain rate, the nanocrystalline sample had lower elastic modulus than submicron grained sample. This decrease has been already observed in the nanocrystalline metal materials with relatively small grains (5–30 nm) [19,20]. The reason will be explained as follows.

3.3 Mechanism for decrease in elastic modulus of nanocrystalline cemented carbide

The elastic behavior of the cemented carbides can be predicted based on the simplified structural model, which assumes that WC particles are embedded in the continuous cobalt matrix. Paul's "strength of materials" formula [2] is

$$E = \frac{E_{Co} + (E_{WC} - E_{Co})\phi_{Co}^{2/3}}{E_{Co} + (E_{WC} - E_{Co})\phi_{WC}^{2/3}(1 - \phi_{WC}^{1/3})} E_{Co} \quad (5)$$

where E , E_{Co} and E_{WC} are the elastic moduli of the cemented carbide, Co phase and WC phase, respectively. ϕ_{Co} and ϕ_{WC} are the volume fractions of Co and WC, and $\phi_{Co} + \phi_{WC} = 1$. For the WC–10Co cemented carbide, $\phi_{Co} = 16.32\%$ and $\phi_{WC} = 83.68\%$.

Seen from Eq. (5), the elastic modulus of the WC–Co cemented carbide is the function of E_{WC} and E_{Co} for a fixed Co content. This indicates that all the reasons affected the atoms equilibrium positions, the bonding forces between the atoms, and lattice constant of the elementary cell.

Generally, the elastic moduli of WC and Co phases are considered as stable values. However, there are two types of Co crystal structures, i.e. face-centered cubic (fcc) and hexagonal close-packed (hcp). It was reported that E_{Co} decreases when the cobalt transforms from fcc to hcp structure [3]. The phase constitutions of the prepared cemented carbides with nanocrystalline and submicron grain structures are shown in Fig. 8. The content ratio of the hcp and fcc structure cobalt phase in the nanocrystalline WC–Co cemented carbide is more than that in the submicron grain sample. The elements in the powder, such as W, C, V and Cr, hardly dissolve in the binder phase during SPS, which may affect the crystal structure of Co phase.

Figure 9 shows the microstructures of the prepared nanocrystalline WC–Co bulk sample. The Co phase with different crystal structures can be indexed by the nanobeam electron diffraction (NBED) patterns. The fcc and hcp cobalt phases are marked as "1" and "2", respectively. It is estimated that there is more than 30% cobalt phase having the hcp structure. This result is consistent with the XRD result in Fig. 8(a). Therefore, the different content ratios of hcp and fcc cobalt phase caused by SPS and sinter-HIP methods may result in the difference of the elastic modulus.

Moreover, the Co mean free path is about 45 nm in nanocrystalline sample with a mean WC grain size of 90 nm. A separate Co zone contains different Co phases (as shown in Fig. 9(b)). Even in a single phase zone, it may contain several Co grains. Therefore, the grain size (22.5 nm) of the Co phase is less than the half of the Co mean free path. If we assumed that WC and Co grains are all spherical, the interface area of cemented carbides (A_f) in unite volume can estimated as follows:

$$A_f = V_{WC-Co} \cdot (1 - \phi_{Co}) / V_{WC} \cdot A_{WC} + V_{WC-Co} \cdot \phi_{Co} / V_{Co} \cdot A_{Co} \quad (6)$$

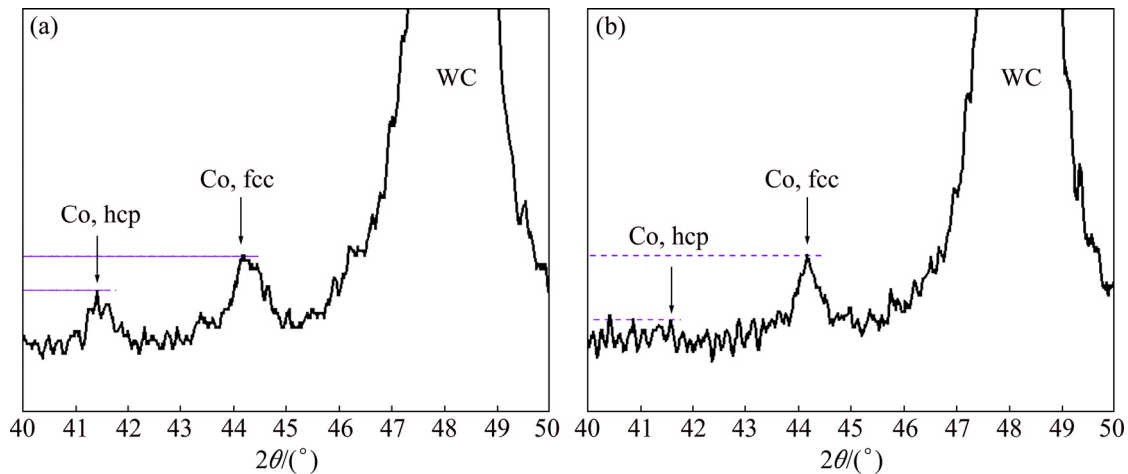


Fig. 8 XRD patterns on Co phase in prepared cemented carbides: (a) Nanocrystalline sample; (b) Submicron grain sample prepared by sinter-HIP

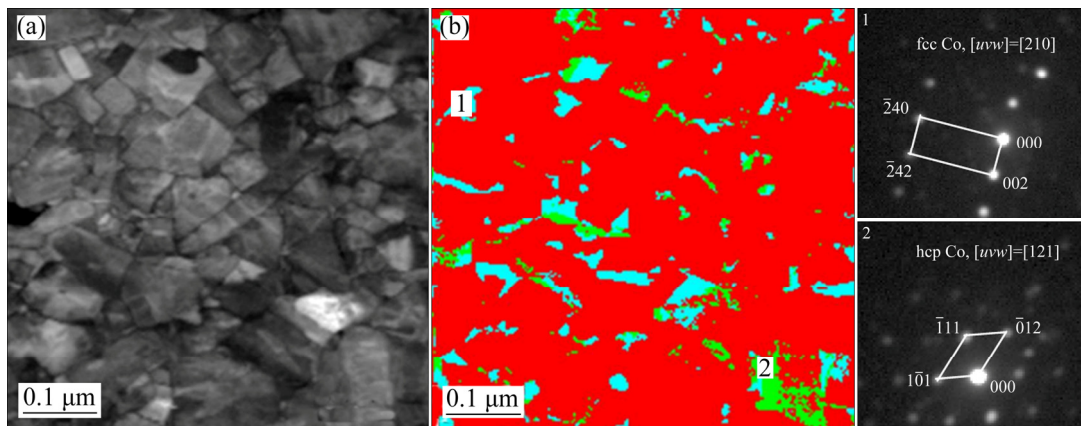


Fig. 9 Microstructures of prepared nanocrystalline WC–Co cemented carbide: (a) TEM image; (b) Distribution of Co phase (1—fcc cobalt, 2—hcp cobalt) (Insert: NBED patterns of individual grains and indexing)

where V_{WC-Co} is the volume of the bulk material; φ_{Co} is the volume fraction of Co phase, and for WC–10Co sample, $\varphi_{Co}=16.32\%$; V_{WC} and V_{Co} are the volumes of the WC grain and Co grain, respectively; A_{WC} and A_{Co} are the surface (the interface) areas of the WC grain and Co grain, respectively. When the grain sizes of Co are 20 and 145 nm in nanocrystalline material and submicron grained material, respectively, the area of interfaces in the nanocrystalline material is seven times as large as that in the submicron grained material. It is well known that atoms in interfaces have larger potential energy than in grains. When the external stress is applied, they easily displace from one place to another, and thus have less contribution to the elasticity compared with that of the atoms inside grains [21,22].

According to the above discussion, the cobalt phase change and the increase of volume fraction of interface in the nanocrystalline cemented carbide are the key factors that result in the decrease of the elastic modulus.

3.4 Application of elastic modulus of nanocrystalline cemented carbide

Figure 3 also shows the energy generated by indenter during loading. Total mechanical energy (W_t) can be shown as

$$W_t = W_p + W_e \quad (7)$$

where W_p and W_e are energies converted to plastic and elastic deformation of the material, respectively. After unloading, only W_p and one part of W_e are transferred to the energy of the material. That is to say, the other part of W_e is dissipated during the indentation process. Under the same indentation depth h , the residual depth h_r increases with increasing elastic modulus E . And according to Eq. (1) and Eq. (2), unloading load P , as well as W_e , decreases with increasing elastic modulus E . The similar result was reported by BAO et al [23] that the higher the value of E_r^2/H (according to Eq. (3), E_r is proportion to E) is, the larger the capacity of energy dissipation is. And SEBASTIANI et al [24] show that the

coefficient of the fracture toughness by nanoindentation method on pillar is proportion to E/H . Therefore, the elastic modulus of the material affects the energy dissipation, thus the service property, especially the toughness, even the service life. The nanocrystalline cemented carbide has a higher hardness and a lower elastic modulus, and it tends to have a relatively low fracture toughness.

4 Conclusions

1) The reliable value of elastic modulus for the nanocrystalline cemented carbide was obtained by measuring the elastic modulus data by CSM method of the nanoindentation technology and averaging these data with a low standard derivation (<5%).

2) The nanocrystalline cemented carbide has a relatively low modulus, compared with the submicron grained cemented carbides prepared by SPS and sinter-HIP. It was caused by a high fraction of hcp cobalt and interface area in the nanocrystalline cemented carbide.

3) Elastic modulus of nanocrystalline and conventional cemented carbides increases with the increase of the strain rate.

References

- [1] RYU T, HWANG K S. Synthesis, sintering and mechanical properties of nanocrystalline cemented tungsten carbide—a review [J]. *International Journal of Refractory Metals and Hard Materials*, 2009, 27: 288–299.
- [2] PAUL B. Prediction of elastic constants of multiphase materials [J]. *Transactions Metallurgy Society AIME*, 1960, 218: 36–41.
- [3] HASHIN Z, SHTRIKMAN S. A variational approach to the theory of the elastic behavior of multiphase materials [J]. *Journal of the Mechanics and Physics of Solids*, 1963, 11: 127–140.
- [4] DOI H, FUJIWARA Y, MIYAKI K, OOSAWA Y. A systematic investigation of elastic moduli of WC–Co alloys [J]. *Metallurgical Transactions*, 1970, 1: 1417–1425.
- [5] LIU X M, SONG X Y, WEI C B, GAO Y, WANG H B. Quantitative characterization of the microstructure and properties of nanocrystalline WC–Co bulk [J]. *Scripta Materialia*, 2012, 66: 825–828.
- [6] SONG X Y, GAO Y, LIU X M, WEI C B, WANG H B, XU W W. Effect of interfacial characteristics on toughness of nanocrystalline cemented carbides [J]. *Acta Materialia*, 2013, 61: 2154–2162.
- [7] WANG X, FANG Z Z, SOHN H Y. Grain growth during the early stage of sintering of nanosized WC–Co powder [J]. *International Journal of Refractory Metals and Hard Materials*, 2008, 26: 232–241.
- [8] ZHANG M J, LI F G, WANG L, WANG S Y. Investigations of inhomogeneous mechanical properties and plastic deformations in HIPed P/M nickel-base superalloy FGH96 by using micro-indentation methods [J]. *Materials Science and Engineering A*, 2012, 556: 233–245.
- [9] HOU L Z, WANG S L, CHEN G L, HE Y H, XIE Y. Mechanical properties of tungsten nanowhiskers characterized by nanoindentation [J]. *Transactions of Nonferrous Metals Society of China*, 2013, 23: 2323–2328.
- [10] GHIDELLI M, SEBASTIANI M, COLLET C, GUILLEMET R. Determination of the elastic moduli and residual stresses of freestanding Au–TiW bilayer thin films by nanoindentation [J]. *Materials & Design*, 2016, 106(15): 436–445.
- [11] OLIVER W C, PHARR G M. Measurement of hardness and elastic modulus by instrumented indentation: Advances in understanding and refinements to methodology [J]. *Journal of Materials Research*, 2004, 19(3): 3–20.
- [12] GHAMARIAN I, LIU Y, SAMIMI P, COLLINS P. C. Development and application of a novel precession electron diffraction technique to quantify and map deformation structures in highly deformed materials—as applied to ultrafine-grained titanium [J]. *Acta Materialia*, 2014, 79 (15): 203–215.
- [13] OLIVER W C, PHARR G M. Improved technique for determining hardness and elastic modulus using load and displacement sensing indentation experiments [J]. *Journal of Materials Research*, 1992, 7(6): 1564–1583.
- [14] GOLOVCHAN V T. On the thermal residual microstresses in WC–Co hard metals [J]. *International Journal of Refractory Metals and Hard Materials*, 2007, 25: 341–344.
- [15] CAI J, LI F G, LIU T Y, CHEN B, HE M. Constitutive equations for elevated temperature flow stress of Ti–6Al–4V alloy considering the effect of strain [J]. *Materials & Design*, 2011, 32(3): 1144–1151.
- [16] GENGA R M, AKDOGAN G, WESTRAADT J E, CORNISHA L A. Microstructure and material properties of PECS manufactured WC–NbC–Co and WC–TiC–Ni cemented carbides [J]. *International Journal of Refractory Metals and Hard Materials*, 2015, 49: 240–248.
- [17] OKAMOTO S, NAKAZONO Y, OTSUKA K, SHIMOITANI Y, TAKADA J. Mechanical properties of WC/Co cemented carbide with larger WC grain size [J]. *Materials Characterization*, 2005, 55: 281–287.
- [18] TOPOLSKI K, BRYNK T, GARBACZ H. Elastic modulus of nanocrystalline titanium evaluated by cyclic tensile method [J]. *Archives of Civil and Mechanical Engineering*, 2016, 16: 927–934.
- [19] KUAN S Y, HUANG J C, CHEN Y H, CHANG C H, HSIEH C H, WANG J H, NIAN Y C, JU S P, NIEH T G, CHEN S H, HWANG Y M. Extended elastic region in nanocrystalline HCP and FCC metals under nano-tension loading [J]. *Materials Science and Engineering A*, 2015, 646 (14): 135–144.
- [20] ZHOU Y, ERB U, AUST K T, PALUMBO G. The effects of triple junctions and grain boundaries on hardness and Young's modulus in nanostructured Ni–P [J]. *Scripta Materialia*, 2003, 48(6): 825–830.
- [21] LATAPIE A, FARKAS D. Effect of grain size on the elastic properties of nanocrystalline α -iron [J]. *Scripta Materialia*, 2003, 48(5): 611–615.
- [22] CHEN Y, SCHUH C A. Contribution of triple junction to the diffusion anomaly in nanocrystalline materials [J]. *Scripta Materialia*, 2007, 57: 253–256.
- [23] BAO Y W, WANG W, ZHOU Y C. Investigation of the relationship between elastic modulus and hardness based on depth-sensing indentation measurements [J]. *Acta Materialia*, 2004, 52(18): 5397–5404.
- [24] SEBASTIANI M, JOHANNIS K E, HERBERT E G, PHARR G M. Measurement of fracture toughness by nanoindentation methods: Recent advances and future challenges [J]. *Current Opinion in Solid State and Materials Science*, 2015, 19(6): 324–333.

纳米硬质合金的弹性模量

刘雪梅¹, 王海滨¹, 宋晓艳¹, Riccardo MOSCATELLI²

1. 北京工业大学 材料科学与工程学院, 北京 100124;

2. Engineering Department, University of Rome “ROMA TRE”, 00146 Rome, Italy

摘要: 本文的研究目的是获得纳米晶 WC-Co 硬质合金的弹性模量, 并分析其弹性模量不同于常规微米硬质合金的原因。采用放电等离子烧结(SPS)方法制备纳米晶硬质合金, 分别采用 SPS 烧结和低压烧结(sinter-HIP)制备常规微米晶硬质合金。烧结试样的显微组织和 WC 晶粒尺寸采用 X 射线衍射技术、扫描电镜、透射电镜及旋进电子衍射技术进行表征。弹性模量采用纳米压痕技术中的连续刚度法进行测量, 并取其稳定区域的平均值得到。结果表明, 与 SPS 制备的微米级硬质合金相比, 纳米晶 WC-Co 硬质合金的弹性模量较小, 可能与界面含量增多和放电等离子烧结过程的快速加热和冷却造成合金钴相中 hcp-Co 含量增多有关。

关键词: 纳米硬质合金; 弹性模量; 纳米压痕; 放电等离子烧结; 钴相

(Edited by Bing YANG)